A DFT Study of the Low-Lying Singlet Excited States of the All-Trans Peridinin in vacuo

Riccardo Spezia,[†] **Costantino Zazza,**[‡] **Amedeo Palma,**[§] **Andrea Amadei,**[∥] **and Massimiliano Aschi*,**[⊥]

Dipartimento di Chimica, Università di Roma "La Sapienza", P.le Aldo Moro 5, 00185 Roma, Italy, and Départment de Chimie, CNRS UMR 8640 PASTEUR, Ecole Normale Supérieure, 24 rue Lhomond, 75231 Paris Cedex 05, France, Consorzio interuniversitario per le Applicazioni di Supercalcolo Per Università e Ricerca (CASPUR), via dei Tizii 6b, 00185 Roma, Italy, Istituto per lo Studio dei Materiali Nanostrutturati (CNR-ISMN), via Salaria, Km 29.3, 00016 Monterotondo S. (Roma), Italy, Dipartimento di Scienze e Tecnologie Chimiche, Università di Roma "Tor Vergata", via della Ricerca Scientifica 1, 00133 Roma, Italy, and Dipartimento di Chimica, Ingegneria Chimica e Materiali, Università de l'Aquila, via Vetoio (Coppito 1), 67010 l'Aquila, Italy

Received: January 27, 2004; In Final Form: June 4, 2004

The electronic properties of peridinin (Per) are investigated using density functional theory (DFT) with a time dependent (TD) treatment for transitions from the ground state to the low-lying electronic excited states. The use of a TD-DFT approach was first tested on the simpler β-carotene molecule in order to see the performances of different functionals. It turns out from the present study that a TD-DFT approach provides a rather good qualitative picture for the electronic properties of this system for which the use of highly correlated ab initio methods with the needed prescriptions, for example, a large enough basis set and/or active space, is still prevented by its large dimension. The vertical transitions of Per obtained in vacuo using TD-DFT are in good agreement with experimental data available in a nonpolar solvent like *n*-hexane. Vertical energies obtained for the minimum energy structure of Per were also refined, spanning the Per in vacuo conformational space using ab initio molecular dynamics on its ground state hypersurface. These calculations also confirm the reliability of TD-DFT calculations at least on properties available from a dynamical sampling, that is, possible state inversion and partial explanation of bandwidth. Hence, combining these results with TD-DFT calculations, it is possible to better understand some spectroscopic properties of peridinin.

1. Introduction

Peridinin (Per, Figure 1) is a fundamental component of the light-harvesting complexes of the photosynthetic dinoflagellates, forming the major component of sea plankton.

These membrane-bound, water-soluble proteins are called peridinin chlorophyll-*a* proteins (PCPs) and contain an unusually large peridinin-to-chlorophyll ratio.[1,2] The presence of peridinin molecules in the PCPs enables the organism to collect light in the visible spectral region where chlorophyll poorly absorbs. Several experimental results show that excitation is transferred directly from peridinin to chlorophyll in the complex.[3] The role of the PCP complex is aimed to finally transfer the excitation mainly to the antenna core complexes of photosystem II (PSII). The peridinins of PCPs are also able to play a photoprotective role by efficient quenching of the chlorophyll triplet states, which may occasionally be populated, thus preventing the formation of the highly toxic singlet oxygen.[2,4]

Stimulated by the solution of the X-ray structure of PCP from *Amphidinium carterae* at a resolution of 2.0 Å,[1] several spectroscopic investigations on Per in PCP have been recently
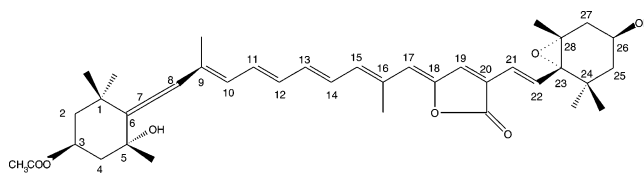

Figure 1. Structure of the all-trans Peridinin with the atom numbering adopted.

performed,[5−10] showing that, together with a basic spectroscopy similar to that of the typical carotenoids, such as β-carotene, some unusual photophysical properties are present, likely due to the presence of a lactone ring along the polyene backbone of peridinin, breaking the C_{2h} symmetry.[11] For common carotenoid molecules, the singlet excited state reached after photon absorption is known to be the upper S_2 state rather than the lower S_1 state for which the oscillator strength is very small (it is expected to be zero in the case of symmetric polyene molecules). The forbidden nature of S_1 leads to a very weak emission from this state. On the other hand, the S_2 state is characterized by a rapid internal conversion to the S_1 state. After photon absorption, Per also reaches the upper S_2 state, followed within 50−300 fs by nonradiative decay into the S_1 state.[12,13] The substitutions in the conjugated structure of peridinin result in a weak emission, in vitro, from the S_1 state; however, the absorption transition $S_0 \rightarrow S_1$ has not been observed.

A theoretical analysis of acceptor substituted carotenoids has suggested that charge tranfer states are important in determining the absorption spectra of these molecules with significant

---

* To whom correspondence should be addressed. Phone: +39-0862-433775. Fax: +39-0862-433753. E-mail: aschi@caspur.it.
† Università di Roma "La Sapienza" and Ecole Normale Supérieure.
‡ Consorzio interuniversitario per le Applicazioni di Supercalcolo Per Università e Ricerca (CASPUR).
§ Istituto per lo Studio dei Materiali Nanostrutturati (CNR-ISMN).
∥ Università di Roma "Tor Vergata".
⊥ Università de l'Aquila.

differences between long and short polyenes.[14] In PCP complexes, the S_1 state of peridinins is supposed, owing to its relatively long intrinsic lifetime (1−300 ps), to tranfer the energy to the chlorophyll-*a* (Chl-*a*),[5] although, recently, energy transfer from the S_2 state has also been proven to take place.[11] An intramolecular charge transfer (ICT) excited state has also been proposed to be populated during the nonradiative decay mechanism[15] of peridinin, on the basis of the dependence of the lifetime of the lowest excited singlet state on the polarity of the solvent. The ICT state has been detected via stimulated emission at 950 nm[15] and could be very close in energy to the S_1 state.[6] A complementary picture done by Frank et al.[16] identifies this ICT state as being vibronically accessible to the S_1, 2^1A_g-like, state; that is, in increasingly polar solvents, the potential energy surface of the S_1 state is significantly distorted, owing to mixing with an ICT state. By using the near-IR pump−probe technique, Zigmantas et al. have recently[17] shown that in PCP complexes from *A. carterae* both the S_1 and ICT states are involved in the energy transfer process to Chl-*a* resulting in a 3 ps^{-1} transfer rate. It has been suggested that the importance of the ICT state lies in its capability to enhance the dipole moment of the S_1 state which leads to an increased efficiency in terms of the energy transfer process to Chl-*a*. In other light-harvesting proteins such as the LH2 complex of purple bacteria or the LHCII complex of higher plants, containing rodophin and lutein/violaxantin/neoxantin carotenoids, respectively, the energy transfer path via the S_2 state dominates, even though other states lower in energy such as the S_1, $^1B_u^-$, or twisted *hot* Car S_1 states are always found to be involved in the energy transfer to (B)Chl.[18,19] Zimmerman et al.[20] have reported the two-photon excitation spectrum of peridinin both in benzene and in PCP, showing that the S_1 state is strongly overlapping the S_2 state, suggesting also a possible mixing of these two states.

This large amount of experimental data has called, in the past, for theoretical investigations aimed to better understand the actual nature and the related properties of Per excited states. Unfortunately, for many years, the application of a reliable theoretical approach to this kind of molecule has been prevented by the fact that Per is a large, flexible, and, more importantly, nonsymmetric molecule. As a matter of fact, highly sophisticated ab initio methods, able to investigate excited states, for example, CAS-PT2[21] or EOM-CCSD,[22] were and still are unaccessible for this class of molecules. For these reasons, the only theoretical information which could be accessed for Per was derived by semiempirical calculations.[23] Only recently, it became possible to address highly sized systems with the use of time dependent density functional theory (TD-DFT)[24−27] which has been extensively shown to provide a valid alternative to the above-cited high-level computational methodologies. The only intrinsic limitation of TD-DFT is the necessity of finding the "best" functional for the problem at hand, that is, the functional that seems to provide results closer to the ones obtained from highly sophisticated methods. Concerning Per, very recently, Head-Gordon and co-workers[28] successfully applied TD-DFT for studying the first excited states features carried out for two selected geometries: the minimum energy and one crystal structure.[1] Intriguingly, they found a large dependence of electronic character with relatively slight geometrical deformations, suggesting a similar analysis for other available crystal structures and, more in general, experimental and theoretical confirmations. From this study, it therefore clearly emerges that the main difficulty associated with Per is its intrinsic flexibility which causes rather limited, if not inappropriate, electronic

structure calculations based on a few mechanical minima. In other words, an investigation on the excited state properties should also evaluate how they could be sensitive to the conformational fluctuations of the molecule.[29] Inspired by the above studies, we decided to give our contribution for trying to better clarify the electronic properties of Per basically by readdressing two crucial problems: (i) the choice of a computationally reliable approach and (ii) the identification of the dependence of the character of the electronic states of Per as a function of its conformational accessible configurations. For this reason, in the present investigation, we have initially carried out a series of test calculations on a smaller probe molecule, hexadecaheptaene (HDH). This particular diapocarotene was chosen because of its symmetry and, more importantly, because of the similarity of its conjugated chain with the Per skeleton. Furthermore, its spectroscopic properties are well-known.[30] The vertical excitation energies from the local minimum energy geometry of the ground state to different singlet excited states of HDH were then evaluated through different theoretical approaches in order to select the best computational procedure for Per. Therefore, according to the HDH calibration, the excited states of Per were subsequently investigated. In the final part of the work, we address point (ii) to obtain a more realistic picture of the electronic properties of Per, strictly connected with its functional activity. For this reason, we need a methodology that is able to investigate the accessible configurational space of such a flexible molecule.[31] This is necessary because the high dimensionality of the system does not allow a systematic sampling of the configurational space. For this reason, we improved two molecular dynamics (MD) simulations: a constant energy dynamic reaction path and a constant temperature Car−Parrinello (CP) molecular dynamics simulation. Both MD simulations were performed on the ground state Born−Oppenheimer hypersurface of Per, obtained via an AM1 Hamiltonian for the former and DFT for the latter. By using a limited number of configurations selected from MD calculations, it was possible to better understand some of the spectroscopic features of Per, like the suggested S_1/S_2 state inversion[15] and the (partial) nature of the full width at half-maximum (fwhm).[6] The MD results are also useful to further appreciate the reliability of TD-DFT based calculations for such a kind of systems. The paper is organized as follows: In the next section, we show the methods used to study the vertical transitions (2.1) and ground state dynamics (2.2) of Per. In section 3, the results are presented and discussed in the same order. Finally, general conclusions are exposed, proposing also future perspectives of this work.

2. Methods

2.1. Singlet Excited States. We initially addressed the excited state properties of HDH. The vertical excitation energies from the local minimum energy geometry of the ground state to different singlet excited states of HDH and Per were then evaluated through different theoretical approaches. First, a configuration interaction procedure including only single excitations, that is, CIS, was performed on the Hartree−Fock (HF) minimized structure for HDH using the 3-21G basis set. Complete active space self-consistent field (CASSCF) calculations,[32] with 14 electrons in 10 orbitals forming the active space, were subsequently carried out on the same molecule with a Huzinaga's MIDI basis set of (6s, 3p)/[3s, 2p] quality[33] on the corresponding HF/MIDI optimized geometry. We also carried out multiconfigurational quasi-degenerate perturbation theory (MCQDPT)[34] using the 6-31++g(d,p) basis set and an active space as large as 10 electrons in 10 orbitals.

Low-Lying Singlet Excited States of Peridinin

J. Phys. Chem. A, Vol. 108, No. 32, 2004 **6765**

Finally, the ground state geometries of HDH were optimized using DFT with the hybrid B3LYP functional, which is composed of the exchange functional of Becke[35] and the correlation functional of Lee, Yang, and Parr.[36] The 3-21G basis set was used for this latter calculation.

A time dependent density functional theory (TD-DFT) based approach[37] was finally employed using different functionals on the corresponding ground state minimum energy geometry: SVWN,[38,39] BLYP,[36,40] B3LYP,[35,36,40] and PBE1PBE[41,42,43] functionals. The SVWN functional based on calculations in the local density approximation (LDA) combines the Slater exchange functional, that is, the local spin density exchange,[38] and the Vosko, Wilk, and Nusair[39] correlation functional which essentially fits the uniform electron gas. BLYP is a functional based on the generalized gradient-corrected approximation (GGA), and it is often referred to as a "pure" GGA method. Finally, two hybrid GGA functionals were considered, the popular B3LYP and the promising[44] new PBE1PBE. All the above functionals were used in conjunction with increasingly large basis sets, that is, 3-21G and 6-31+G(d). Hereafter, these calculations will be called TD-SVWN, TD-BLYP, TD-B3LYP, and TD-PBE1PBE, respectively.

For Per, only DFT based calculations were improved, since the high degree of complexity (in terms of the number of electrons and reliable number of conformations to be used) causes an important limitation in the available electronic structure approach. For this reason, only the 3-21G basis set was used to carry out TD-DFT calculations on Per.

2.2. Dynamics of the Singlet Ground State. Singlet Per is expected to fluctuate in thermal conditions. Therefore, the calculation of the vertical energy, only considering the absolute minimum on the Born−Oppenheimer hypersurface of the ground state, could be affected by a relatively large degree of incompleteness. Rather, the occurrence of different conformers which could heavily affect both the value of the absorption wavelength and the corresponding oscillator strength should be taken into account. At this end, several procedures can be alternatively followed. In the present study, the configurational space actually spanned by the singlet Per in vacuo has been sampled through a dynamic reaction path (DRC)[45] calculation in the microcanonical ensemble, that is, constant energy and angular momentum. In such a method, the molecule nuclear degrees of freedom are allowed to classically evolve into the electronic energy hypersurfaces defined step-by-step through a semiempirical AM1 Hamiltonian.[46] The trajectories were initiated in the correspondence of potential energy AM1 minima propagated up to 20 ps with the initial atomic velocities adjusted to give an average temperature of 350 K. The velocity Verlet algorithm was used with a time step of 0.1 fs. The implementation of Gordon and Taketsugu was adopted to this purpose.[45] The trajectory was therefore analyzed using the principal component analysis (PCA) method.[47] In this context, the PCA method should allow a good estimation of the large amplitude vibronic effects for a large and flexible system like Per. To perform the PCA, the equilibrated portion (∼15 ps) of the DRC simulation was used for building the covariance matrix **C** of the positional fluctuations of carbon and oxygen atoms. It must be reminded that the generic element of the covariance matrix is

$$C_{ij} = \langle (x_i(t) - \langle x_i \rangle)(x_j(t) - \langle x_j \rangle) \rangle \qquad (1)$$

The ortonormal set of eigenvectors obtained from the diagonalization of **C** provides a new set of coordinates, and the modes associated with the largest eigenvalues describe the significant motion of the molecule.

In the final step, the trajectory has been projected on the first two eigenvectors obtained from the diagonalization of the covariance matrix. Such an operation gives rise to a series of structures among which we have considered the structures corresponding to the maximum and the minimum of the essential eigenvectors. In correspondence with these latter structures, TD-DFT calculations were performed with the SVWN functional. Note that in this study we are sampling the accessible configurational space of Per, looking at vertical transitions corresponding to different structures in different regions of the configurational space. All the above quantum chemical calculations were performed with the Gaussian 98[48] and GAMESS US[49] packages, whereas the PCA was done using the GROMACS package utilities.[50]

Since the DRC calculations are performed at constant energy and the limited length of the simulation does not allow a microcanonical sampling for describing a constant temperature behavior to be considered reliable, we performed a constant temperature MD simulation to confirm the previous results. For this reason, we improved the Car−Parrinello (CP) approach to this system. The trajectories were obtained from a CP molecular dynamics simulation[51−53] of 15 ps at a finite temperature of 300 K. All electronic and ionic degrees of freedom were simultaneously relaxed using a damped MD scheme.[54] The electronic structure calculations were performed within DFT using the generalized gradient-corrected approximation of Perdew, Burke, and Ernzerhof (PBE)[42,55,56] for exchange and correlation energy. We adopted a plane wave pseudopotentials (PPs) expansion using ultrasoft PPs for O, C, and H atoms.[57] The calculations have been performed in an orthorhombic cell subject to periodic boundary conditions. The cell was chosen large enough to avoid molecular interactions between periodic images. The Brillouin zone was sampled using the Γ point. After a full relaxation (forces <10^{-4} au) at 0 °C, we obtained a Per local minimum structure in excellent agreement with the local minimum geometry found using static calculations in vacuo. Note that the same computational scheme has been successfully applied in previous works of one of us.[58,59]

3. Results and Discussion

3.1. Ground State Optimization. The singlet ground state geometry of Per was optimized using DFT with the B3LYP functional using a 3-21G atomic basis set, providing an absolute minimum corresponding to a pseudo-C_S structure, that is, with the conjugated π-skeleton lying on the same plane formally intersecting both of the cyclic aliphatic terminal groups. Moreover, we also compared the energy minimized B3LYP structure in vacuo with the available X-ray structure obtained for the four different Per molecules in pentachlorophenol (PCP) (Protein Data Bank entry code, 1PPR[1]). In terms of internal coordinates, we could reproduce all the geometrical values with a root-mean-square deviation <1% for the bond lengths and ∼6% for the angles. On the other hand, the actual torsional angles characterizing the B3LYP minimum sharply differ from the above crystallographic structures. This finding can be easily appreciated by inspecting Figure 2, where the absolute deviations of the four crystallographic structures (labeled as Per1, Per2, Per3, and Per4) are reported with respect to the B3LYP absolute minimum. This analysis has been carried out only considering the molecular "backbone", that is, the atoms from 1 to 28 in Figure 1. Note that the largest differences (larger than 0.5 Å) are found only in the terminal cyclohexane ring, with the only
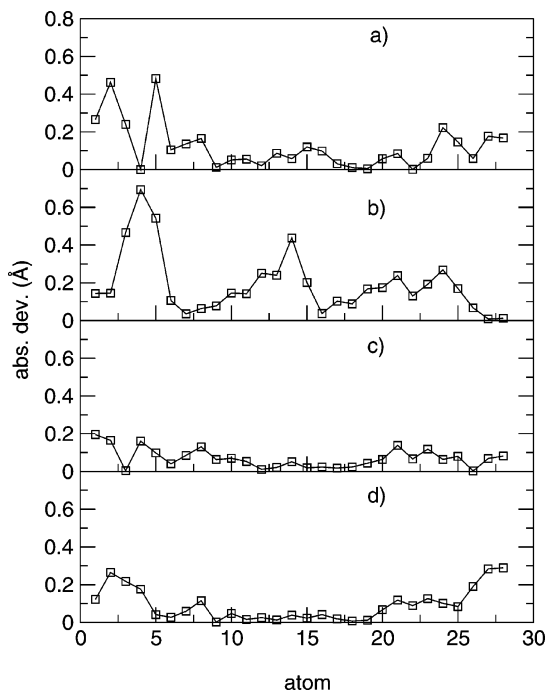
Figure 2. Absolute deviations (in angstoms) of Per1 (a), Per2 (b), Per3 (c), and Per4 (d) with respect to the B3LYP/3-21G absolute minimum.

TABLE 1: Calculated and Experimental Vertical Excitation Energies (in eV) with the Corresponding Oscillator Strengths (in au) for the Absolute Minimum of HDH at Different Levels of Theory

method	S_1	S_2	f_1	f_2
CIS/3-21G	4.16	5.61	2.5	0.0
CASSCF(14, 10)/MIDI	5.64	5.90	0.0	1.5
MCQDPT(10, 10)/6-31++g(d,p)	4.20	4.9	0.0	1.2
TD-B3LYP/3-21G	3.13	3.58	2.0	0.0
TD-B3LYP/4-31G	3.08	3.54	1.7	0.0
TD-B3LYP/6-31+G(d)	3.01	3.50	1.8	0.0
TD-BLYP/3-21G	2.44	2.48	0.0	2.9
TD-PBE1PBE/3-21G	2.91	3.42	3.1	0.0
TD-PBE1PBE/6-31+G(d)	2.79	3.34	3.1	0.0
TD-SVWN/3-21G	2.49	2.52	0.0	3.0
TD-SVWN/6-31+G(d)	2.41	2.43	3.0	0.0
experimental[30]	2.41	3.04		intense

exception being C14 in the conjugated skeleton of Per2. This strengthens the view that the protein environment can have a minor role in determining the static structure of peridinin, while it seems to play a crucial role in its dynamics.[31] The geometry was also optimized, with the same basis set, using the other three functionals, that is, BLYP, PBE1PBE, and SVWN, in order to carry out the related excited state calculations (see below).

3.2. Singlet Excited States. First of all, we selected the most suitable computational strategy by performing excited state calculations on the HDH species, as described in the Methods section. The results are collected in Table 1. As already mentioned, it is known that such a symmetric molecule, which is ^1A_g in the ground state, is not allowed to reach, by photon absorption, the S_1, ^1A_g-like, state. In contrast, the transition to the S_2 , ^1B_u-like, state is allowed. It is also known[27,60] that for a correct treatment of the excited states of these kind of systems, high order excitations and/or electronic correlations cannot be disregarded.

As expected, the configuration interaction performance, that is, the CIS calculations, appears as severely wrong. Not only are the energy ranges quite far from the experimental range, but the order of the states (S_1/S_2) is even inverted. On the other

TABLE 2: Comparison of the Vertical Excitation Energies (in eV) with the Corresponding Oscillator Strengths (in au) for the First Two Excited States of Per Using Different Functionals

method	S_1	S_2	f_1	f_2
TD-BLYP/3-21G	2.06	2.12	2.4	0.4
TD-SVWN/3-21G	2.07	2.23	0.0	2.8
TD-B3LYP/3-21G	2.37	2.94	3.3	0.3
TD-PBE1PBE/3-21G	2.49	3.15	3.6	0.3
experiment[2]	2.07	2.55		intense

hand, the multiconfigurational approach, that is CASSCF, although correctly describes the sequence of the two states, again overestimates the transition energy value. Surprisingly, even the computationally very demanding MCQDPT calculations, although correctly describing the sequence of the states, do actually overestimate their relative energies. It is probably due to some deficiency arising from the relatively small dimension of the active space. Using a correlated approach such as TD-DFT, we can observe an improvement in the values of the energy, with the results being fairly sensitive to the dimension and the quality of the basis set. Recent studies[61] have demonstrated that, for accessing reliable information on low-lying excited states[62] of relatively large molecular systems, the TD-DFT approach, with gradient-corrected nonlocal density approximation, for example the B3LYP functional, provides a very efficient tool. In fact, when a split valence basis set is used in conjuction with polarization and diffusion functions, the energy of the allowed excited state is found to fall close to the correct value of 3.04 eV. Nevertheless, the result is not entirely correct, since this latter transition corresponds to the $S_0 \rightarrow S_1$ transition and not to the $S_0 \rightarrow S_2$ transition, as experimentally observed. In other words, the B3LYP functional, although suitable for reproducing the energy range, appears to overstimate the $S_0 \rightarrow S_1$ transition.

Hence, we tested the performace on HDH of other common functionals: BLYP, PBE1PBE, and SVWN. While PBE1PBE gives results only slightly better than the B3LYP ones, that is, it can reduce the ground state to excited state energy difference but again by "inverting" S_1 and S_2 states, interestingly, the BLYP and SVWN functionals provide a more consistent picture. As a matter of fact, the sequences of the first and second excited states are correctly reproduced, at least, formally, using one basis set, although the absolute values are not in fully quantitative agreement. Anyway, these calculations give very small S_1/S_2 energy differences, and hence, we have uncontrolled oscillations changing the functional and/or basis set in the excited state energies leading to an apparently different sequence of states. Note that the relatively good performance of the SVWN functional confirms the results obtained for small polyenes, being in agreement with highly correlated calculations.[24]

Even if the TD-SVWN approach seems to be a good choice for studying Per, considering results obtained for HDH as well as literature data,[24,25,27,28] we first did a few tests using the four functionals improved for HDH, that is, BLYP, SVWN, B3LYP, and PBE1PBE. In Table 2, we show the first two excited states obtained with these functionals. As we can see from this comparison, excited state transitions seem to be better reproduced using the SVWN functional. Also, the BLYP one fails in this case; although it gives similar energies, it does not provide the correct oscillator strengths. The two "hybrid" GGA functionals seem both to overestimate the transition energies as well as to fail in the state sequence. On the basis of all of these tests, confirming previously reported literature data on such a class

Low-Lying Singlet Excited States of Peridinin

J. Phys. Chem. A, Vol. 108, No. 32, 2004 **6767**

of compounds,[24,25,28] the SVWN functional will be adopted to further investigate the Per properties in this paper. In this case, we considered the first five excited states. The corresponding excitation energies and oscillator strengths, reported in Table 3, are compared with literature data, both calculated[23,28] and experimental.[2] All these states are characterized by a strong degree of mixing (see below), and their character turned out to be very difficult to identify because of the lack of symmetry. In fact, on the basis of a simplified characterization of the electronic transitions in terms of homo (H) and lumo (L), the transitions from the ground state to the first two excited states are basically combinations of H → L and H − 1 → L with a small contribution of H − 3 → L and H → L + 1 (the latter only for the transition to the second excited state). The transition to the third state, as well as to the higher states, was found to be mainly a H − 2 → L transition with a small contribution of H − 3 → L. Note that these results are in qualitative agreement with previous calculations, identifying high degrees of mixing, unusual in linear polyenes but expected in Per because of its substituents. On the basis of the above picture, and on the basis of the nature of the homo, lumo, and related orbitals, all the low-lying transitions appear as involving diffuse π-orbitals extended over all the centers of the conjugated skeleton as well as the lactone ring. The calculated energy of the first excited state (S_1, A_g-like) is in agreement with the experimental value obtained in a nonpolar solvent (*n*-hexane) indirectly from fluorescence emission by Frank and co-workers[2]. To identify the spectral origin in the absence of clear vibronic features in the band profile (as in this case), they used the approach proposed by Cosgrove et al.[63] This approach provides insight into how one might assign the origin of emission of polyenes whose spectra lack resolution in their vibronic features. Note that here and hereafter we used as an experimental reference of our in vacuo calculations the values obtained in *n*-hexane, since, to our knowledge, no in vacuo spectroscopy is reported. Furthermore, the electrostatic influence of *n*-hexane in the Per spectra can be considered negligible.

Also, the allowed S_2 state (B_u-like), lying 2.23 eV above the ground state, is in good agreement with experimental findings (~2.55 eV)[2]. Moreover, all of the upper forbidden states, herein denoted as the S_3, S_4, and S_5 states, were actually found to lie very closely to S_2. Such a finding, denoting a relatively high electronic density of the states, experienced by the system once the S_2 state is vertically reached, can qualitatively explain the relatively short lifetime of the S_2 state which can very easily internally convert into a high number of plausible states. Note that no direct experimental findings are reported for these higher nonaccessible states. Only recent calculations[23,28] have reported these states. From semiempirical (MNDO-PSDCI)[23] calculations, they were identified to be higher in energy, while a similar picture of dense states emerges from TD-DFT based calculations.[28] The nature of this small energy difference is not so clear at this stage. It is interesting to note that both the CASSCF and MCQDPT calculations, previously described, although providing a picture not completely correct in quantitative terms, did not show such a high density of states. Since no direct experiments are present, we should note that this finding can be due to some limitations of the TD-DFT method, for example, the lack of multiple excitations. Moreover, we should note how small modifications in Per geometry produce a nonnegligible effect on excited states, especially on the character of such close states. As we will discuss in the next subsection, the inclusion of Per flexibility will be crucial to understand the properties of the excited states.
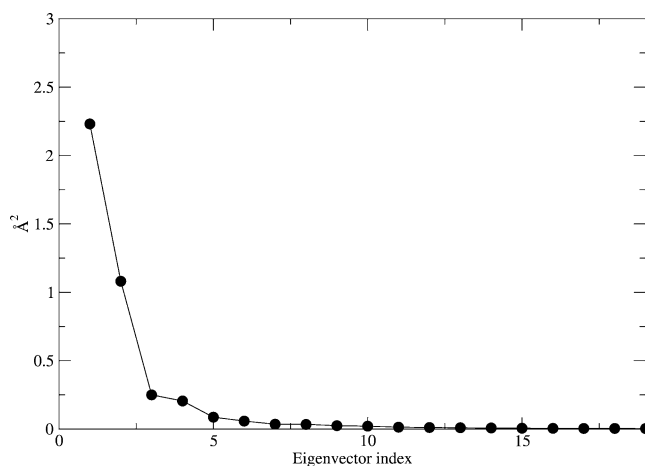

Figure 3. Eigenvalues spectrum obtained from the diagonalization of the covariance matrix from the ground state trajectory.

3.3. Dynamical Sampling. To appreciate the feasible effects of the Per large amplitude motions on its spectroscopical behavior, we also combined a dynamical analysis with the TD-DFT calculations. At this end, the molecular dynamics (MD) ground state Per equilibrated trajectories were analyzed using the principal component analysis (PCA). The eigenvalues obtained from the diagonalization of the covariance matrix (eq 1) for the Per DRC simulation are reported in Figure 3. It is clear that the molecule principal (essential) motion is almost entirely characterized by two modes. The same analysis was performed on the CP molecular dynamics simulation, giving essentially the same results in terms of eigenvalues and eigenvectors. Since the two dynamics seem to be very similar, we used only the first one (the DRC one) for the TD-DFT calculations. The projection of the trajectories along these two principal directions basically shows an out-of-plane rotation along the C14−C15 bond leading to a trans−cis isomerization (the first one) and to a coupled oscillation around the C14−C15 and C8−C9 bonds (the second one). Both of the above modes also showed a rather marked out-of-plane fluctuation of the overall carbon skeleton. Since the principal aim of the present work is to clarify the low-lying excited states of Per, a deeper analysis of its ground state dynamics will be presented elsewhere.[64] It is only interesting to note here that the general features of the essential eigenvectors (i.e., principal motions) fully reflect the distortion observed in the X-ray structures.

In correspondence to the above structures, we therefore carried out the TD-SVWN/3-21G calculations. These calculations should provide, in principle, the effect of the large amplitude fluctuations on the spectroscopical features such as excitation energies and transition moments. The above analysis carried out on the first three excited states is schematized in Figure 4, while, in Table 4, we present the excited state energies obtained for the first five states on the same structures. In Figure 4a, we have reported the projection along the first eigenvector of the excitation energies associated to the transitions $S_0 → S_1$, $S_0 → S_2$, and $S_0 → S_3$. The names as well as the character of the excited states, that is, S_1, S_2, and S_3, are referred to as the first, second, and third excited states obtained from the TD-DFT calculations carried out on the absolute minimum geometry. From this figure, it can be seen that, in correspondence with the value −1 of the associated eigenvector, the lowest state turns out to be the allowed one. Such a finding, although surprising and, at the same time, very difficult to predict, is however very interesting and apparently in agreement with some experimental observations according to which, in some cases,
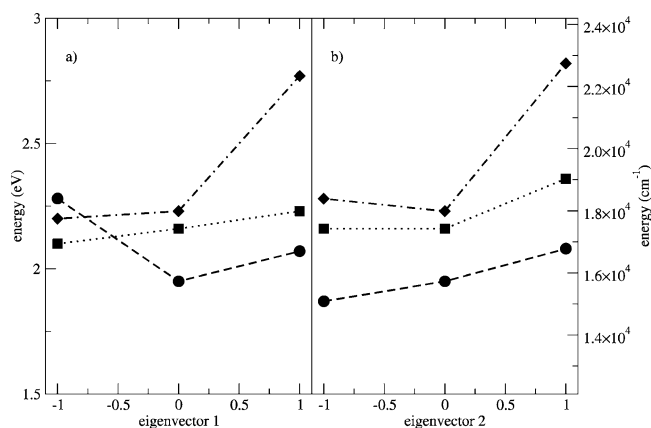
Figure 4. Excitation energies along the first (a) and second (b) eigenvector. The spectroscopically allowed $S_0 \rightarrow S_2$ transition is reported by the dotted line, whereas the $S_0 \rightarrow S_1$ and $S_0 \rightarrow S_3$ transitions are reported by the dashed and dot−dashed lines, respectively.

TABLE 3: Comparison of the Vertical Excitation Energies[a] (in eV) with the Corresponding Oscillator Strengths (in au) of the TD-DFT Calculations (This Work), MNDO-PSDCI Calculations,[23] TD-DFT/TDA Calculations,[28] and Experiments[2]

	E/TD-DFT	*E*/MNDO-PSDCI	*E*/TD-DFT/TDA	*E*/expt
S_1	2.07	1.96	2.26	2.07
	(0.03)	(0.23)	(1.00)	(absent)
S_2	2.23	2.39	2.41	2.55
	(2.81)	(1.68)	(1.98)	(intense)
S_3	2.28	2.80	2.65	
	(0.01)	(0.23)	(0.08)	
S_4	2.29	3.35	2.69	
	(0.00)	(not reported)	(2.49)	
S_5	2.31	3.60		
	(0.31)	(not reported)		

[a] The calculated values correspond to their own fully optimized structures.

TABLE 4: Peridinin Excited State Energies (in eV) Extracted From DRC-MD[a]

		eig 1		eig 2	
state	zero	max	min	max	min
S_1 (A_g-like)	1.95	2.07	2.28	2.08	1.87
S_2 (B_u-like)	2.16	2.23	2.10	2.36	2.16
S_3	2.23	2.77	2.20	2.82	2.28
S_4	2.29	2.84	2.42	2.86	2.35
S_5	2.31	2.92	2.44	2.92	2.50

[a] Max, min, and zero correspond to $+1$, -1, and 0 along both eigenvectors, respectively.

a low-lying ghost state is observed.[15] Nicely, recent semiempirical calculations of Per in the environment of PCP also reported the possibility of such an inversion of the first two excited states.[23] On the other hand, from part b of Figure 4, it can be easily seen that, although the values of the absolute energy gap are slightly affected by the conformational changes, their relative values remain basically unchanged. In other words, the second eigenvector does only alter the width of the UV spectrum which, on the basis of our calculations, is expected to be as large as 0.2 eV (corresponding to ~60 nm). This value is also in good qualitative agreement with experiments reporting a fwhm of ~0.5 eV.[6]

It also should be noted that we found an S_3 state very close to the S_2 one only in the equilibrium configuration, like in calculations reported for the minimized geometry, while along the eigenvectors this quasi-degeneracy can be lost, producing a difference in energy of ~0.5 eV. As can be further noted from

Table 4, the higher excited states (from S_3 to S_5) largely oscillate as a function of the internal Per motion. This evident property, while it bridges the small gap with other calculated data,[23,28] also leaves open the question of the location, and hence the role, of these states. Further experiments with combined theoretical investigations can be, of course, crucial to address this problem.

4. Conclusions and Outlooks

In this work, we provide a TD-DFT based picture of the singlet excited states of peridinin (Per). The justification of using in our work TD-DFT in connection with the SVWN functional is based on benchmark calculations done on the rather similar β-carotene and the hexadecaheptene (HDH) as well as on literature inspection.[24,25,28]

In the case of HDH, we noted that high-level ab initio approaches, such as CASSCF and MCQDPT, do not provide a totally correct picture, probably due to the dimension of the system that forces one to use a relatively small atomic basis set and/or a not large enough active space, and one should employ CAS-PT2 calculations to have the correct energies and sequence of states. We also noted that hybrid GGA functionals do not provide accurate enough results. Pure GGA (BLYP) and LDA (SVWN) based functionals seem to provide a better picture with respect to the one obtained from hybrid functionals. In fact, even if they are not fully and always in agreement with experimental data, they can provide generally a picture not so far from the correct one obtained via CAS-PT2 calculations. Anyway, we have to note that TD-DFT methods can suffer from the problem of underestimating the energy gap between close excited states. Keeping in mind the well-known intrinsic limitations of TD-DFT calculations, results on HDH are useful to see that for this kind of system probably the best functional is the SVWN one. This is important especially when the molecule under investigation is a complex one, that is, it has a large number of atoms and any symmetry, like Per, for which CAS-PT2 calculations are still undoable.

A similar picture was obtained in the case of Per, where the best functional, among the four tested, seems to be the SVWN one, confirming recent calculations done by Head-Gordon and co-workers.[28] This approach can provide us with a view of the low-lying excited states of Per that is in very good agreement with experimental data as well as with recent semiempirical calculations. Note that this good performance of TD-DFT should be considered somewhat surprising, particularly because the singlet 2^1A_g-like state contains substantial contributions with a double excitation character and TD-DFT is an explicitly one-electron description where higher excitations are treated only implicitly by dressing the response matrix with the effects of electron correlation. From the present calculations, the dark S_1 excited state was located 2.07 eV above the ground state, confirming fluorescence studies, while the spectroscopically allowed S_2 state was found at 2.23 eV with a large oscillator strength. Moreover, we found several nonactive states a few electonvolts above S_2. These states could be accessible via nonradiative transitions from S_2, giving a partial explanation of the short lifetime of the S_2 state. A dynamical picture of this S_2 state could be useful to better characterize the photochemistry of peridinin.

In this in vacuo study, we identify and characterize a spectroscopically forbidden S_1 state, known to be strictly related to an ICT state.[16] Of course, the inclusion of a polar solvent will be essential to better characterize this state, especially for its dynamics. This feature, even if very interesting and intriguing,

is beyond the aim of this work. Anyway, this work can be a first and necessary step in that direction. In fact, a clear in vacuo description is needed for further studies using both a discrete and continuum solvent description.[65-69]

We refined our calculations based on vertical transitions from the ground state potential energy minimum spanning the conformational space accessible to Per in its ground state via MD simulations. This so-called "dynamical refining" is more crucial in the Per case, since the reliability of the TD-DFT calculations, noted to be largely geometry dependent, cannot be honestly and definitively justified only taking into account the minimum energy geometry. In this sense, our MD simulations deal with an accurate validation of the computational approach and they can provide a complementary view of Per photophysics that is emerging from considering the different crystal structures available.[28] By coupling molecular dynamics with the PCA and TD-DFT calculations, we were also able to note that an interchange between S_1 and S_2 is allowed. This particular property is found in a region, or at least a structure, located at an extreme of the first eigenvector of Per. Since first eigenvectors correspond to larger vibronic motions, that is, low frequency motions, the corresponding structures are very difficult to find with standard procedures, expecially for such a large molecule. Also, the second eigenvector is related to the Per spectroscopic properties. It seems to have a large, although not unique, role in determining the fwhm of the spectrum. Anyway, a further analysis on the Per ground state dynamics in connection with all essential motions, or the equivalent normal mode, and devoted to better clarify the Per conformational dynamics, is needed and is actually under investigation in our group.[64] As noted above, from such calculations, it clearly emerges that the electronic features of a highly fluctuating molecule like Per cannot be addressed by only considering the potential energy absolute minimum. Rather, the presence of other conformers induced by the large internal motions or, more generally, by the environment, for example, solvent or protein, can alter, in some cases also dramatically, the electronic properties and therefore the biological role of Per. This dynamical refining strengthens the idea that TD-DFT based calculations for large biological chromophores can be useful for understanding their complex photophysics. In fact, the relatively small (in comparison with highly correlated methods) computational effort needed for such calculations is not always basic for single point calculations, but also, and especially, because they can be successfully coupled with conformational sampling techniques.

Finally, we would like to point out that these first calculations, reporting vertical (Franck−Condon) transitions for different accessible configurations, can be a useful starting point to better investigate the photochemistry of Per. Of course, for this reason, nonadiabatic effects should be included to better handle the excited state properties. In particular, it could be interesting to conduct further studies on the S_2 state, where higher dark excited states seem to be very close to this state and conical intersections between excited states can influence dramatically its dynamical behavior.

References and Notes

(1) Hofmann, E.; Wrench, P. M.; Sharples, F. P.; Hiller, R. G.; Welte, W.; Diederichs, K. *Science* **1996**, *272*, 1788−1791.

(2) Bautista, J. A.; Hiller, R. G.; Sharples, F. P.; Gosztola, D.; Wasielewski, M.; Frank, H. A. *J. Phys. Chem. A* **1999**, *103*, 2267−2273.

(3) Larkum, T. *Trends Plant Sci.* **1996**, *1*, 247−248.

(4) Mathews-Rode, M. M. *Carotenoids in erythropoietic protoporphyria and other photosensitivity desease*; New York, 1993.

(5) Akimoto, S.; Takaichi, S.; Ogata, T.; Nishimura, Y.; Yamazaki, I.; Mimuro, M. *Chem. Phys. Lett.* **1996**, *260*, 147−152.

(6) Bautista, J. A.; Connors, R. E.; Raju, B. B.; Hiller, R. G.; Sharples, F. P.; Gosztola, D.; Wasielewski, M.; Frank, H. A. *J. Phys. Chem. B* **1999**, *103*, 8751−8758.

(7) Osuka, A.; Kume, T.; Haggquist, G. W.; Jaforvi, T.; Lima, J. C.; Melo, E.; Naqvi, K. R. *Chem. Phys. Lett.* **1999**, *313*, 499−504.

(8) Carbonera, D.; Giacometti, G.; Segre, U.; Angerhofer, A.; Gross, U. *J. Phys. Chem. B* **1999**, *103*, 6357−6362.

(9) Carbonera, D.; Giacometti, G.; Segre, U.; Hofmann, E.; Hiller, R. G. *J. Phys. Chem. B* **1999**, *103*, 6349−6356.

(10) Kleima, F. J.; Wendling, M.; Hofmann, E.; Peterman, E. J. G.; van Grondelle, R.; van Amerongen, H. **2000**, *39*, 5184−5195.

(11) Krueger, B. P.; Lampoura, S. S.; van Stokkum, I. H. M.; Papagiannakis, E.; Salverda, J. M.; Gradinaru, C. C.; Rutkauskas, D.; Hiller, R. G.; van Grondelle, R. *Biophys. J.* **2001**, *80*, 2843−2855.

(12) MacPherson, A. N.; Gilibro, T. *J. Phys. Chem. A* **1998**, *102*, 5049−5058.

(13) Mimuro, M.; Akimoto, S.; Takaichi, S.; Yamaaki, I. *J. Am. Chem. Soc.* **1997**, *119*, 1452−1453.

(14) Tretiak, S.; Chernyak, V.; Mukamel, S. *J. Am. Chem. Soc.* **1997**, *119*, 11408−11419.

(15) Zigmantas, D.; Polivka, T.; Hiller, R. G.; Yartsev, A.; Sundstroem, V. **2001**, *105*, 10296−10306.

(16) Frank, H. A.; Bautista, J. A.; Josue, J.; Pendon, Z.; Hiller, R.; Sharples, F.; Gosztola, D.; Wasielewski, M. R. *J. Phys. Chem. B* **2000**, *104*, 4569−4577.

(17) Zigmantas, D.; Hiller, R. G.; Sundstroem, V.; Polivka, T. *Proc. Natl. Acad. Sci. U.S.A.* **2002**, *99*, 16760−16765.

(18) Papagiannakis, E.; Kennis, J. T. M.; van Stokkum, I. H. M.; Cogdell, R. J.; van Grondelle, R. *Proc. Natl. Acad. Sci. U.S.A.* **2002**, *99*, 6017−6022.

(19) Walla, P. J.; Linden, P. A.; Ohta, K.; Fleming, G. R. *J. Phys. Chem. A* **2002**, *106*, 1909−1916.

(20) Zimmermann, J.; Linden, P. A.; Vaswani, H. M.; Hiller, R. G.; Fleming, G. R. *J. Phys. Chem. B* **2002**, *106*, 9418−9423.

(21) Andersson, K.; Malmqvist, P. A.; Ross, B. O.; Sadlej, A. J.; Wolinski, K. *J. Phys. Chem.* **1990**, *94*, 5483−5488.

(22) Stanton, J. F.; Gauss, J. *J. Chem. Phys.* **1995**, *103*, 1064−1076.

(23) Shima, S.; Ilagan, R. P.; Gillespie, N.; Sommer, B. J.; Hiller, R. G.; Sharples, F. P.; Frank, H. A.; Birge, R. R. *J. Phys. Chem. A* **2003**, *107*, 8052−8066.

(24) Hsu, C. P.; Hirata, S.; Head-Gordon, M. *J. Phys. Chem. B* **2001**, *105*, 451−458.

(25) Dreuw, A.; Fleming, G. R.; Head-Gordon, M. *Phys. Chem. Chem. Phys.* **2003**, *5*, 3247−3256.

(26) Fantacci, S.; Migani, A.; Olivucci, M. *J. Phys. Chem. A* **2004**, *108*, 1208−1213.

(27) Hsu, C. P.; Walla, P. J.; Head-Gordon, M.; Fleming, G. R. *J. Phys. Chem. B* **2001**, *105*, 11016−11025.

(28) Vaswani, H. M.; Hsu, C. P.; Head-Gordon, M.; Fleming, G. R. *J. Phys. Chem. B* **2003**, *107*, 7940−7946.

(29) Spezia, R. Computational Studies of the Coupling between Molecular Dynamics and Electronic Properties in Complex Systems. Ph.D. Thesis, Dipartimento di Chimica, Università di Roma "La Sapienza", 2003.

(30) Christensen, R. L.; Goyette, M.; Gallagher, L.; Duncan, J.; DeCoster, B.; Lugtenburg, J.; Jansen, F. J.; van der Hoef, I. *J. Phys. Chem. A* **1999**, *103*, 2399−2407.

(31) Spezia, R.; Aschi, M.; Di Nola, A.; Di Valentin, M.; Carbonera, D.; Amadei, A. *Biophys. J.* **2003**, *84*, 2805−2813.

(32) Roos, B. O. *Adv. Chem. Phys.* **1987**, *69*, 399−427.

(33) Andzelm, J.; Klobulowsky, M.; Radzio-Andzelm, E.; Sakai, Y.; Tatewaki, H. *Gaussian Basis Sets for Molecular Calculations*; Elsevier: Amsterdam, The Netherlands, 1984.

(34) Nakano, H. *J. Chem. Phys.* **1993**, *99*, 7983−7992.

(35) Becke, A. D. *J. Chem. Phys.* **1986**, *84*, 4524−4529.

(36) Lee, C.; Yang, W.; Parr, R. G. *Phys. Rev. B* **1988**, *37*, 785−789.

(37) Hirata, S.; Head-Gordon, M. *Chem. Phys. Lett.* **1999**, *302*, 375−382.

6770 *J. Phys. Chem. A, Vol. 108, No. 32, 2004*

Spezia et al.

(38) Slater, J. C. *Quantum theory of molecules and solids: The self-consistent field for molecules and solids*; McGraw-Hill: New York, 1974; Vol. 4.

(39) Vosko, S. J.; Wilk, L.; Nusair, M. *Can. J. Phys.* **1980**, *58*, 1200−1211.

(40) Becke, A. D. *J. Chem. Phys.* **1993**, *98*, 5648−5652.

(41) Perdew, J. P.; Wang, Y. *Phys. Rev. B* **1992**, *45*, 13244−13249.

(42) Perdew, J. P.; Burke, K.; Ernzerhof, M. *Phys. Rev. Lett.* **1996**, *77*, 3865−3868.

(43) Ernzerhof, M.; Scuseria, G. E. *J. Chem. Phys.* **1999**, *110*, 5029−5036.

(44) Adamo, C.; Barone, V. *Chem. Phys. Lett.* **1999**, *314*, 152−157.

(45) Taketsugu, T.; Gordon, M. S. *J. Phys. Chem.* **1995**, *99*, 8462−8471.

(46) Dewar, M. J. S.; Zoebisch, E. G.; Healy, E. F. *J. Am. Chem. Soc.* **1985**, *107*, 3902−3909.

(47) Amadei, A.; Linssen, A. B. M.; Berendsen, H. J. C. *Proteins* **1993**, *17*, 412−425.

(48) Frisch, M. J.; et al. *Gaussian 98*, revision A.7; Gaussian, Inc.: Pittsburgh, PA, 1998.

(49) Schmidt, M. W.; Baldridge, K. K.; Boatz, J. A.; Elbert, S. T.; Gordon, M. S.; Jensen, J. J.; Koseki, S.; Matsunaga, N.; Nguyen, K. A.; Su, S.; Windus, T. L.; Dupuis, M.; Montgomery, J. A. *J. Comput. Chem.* **1993**, *14*, 1347−1363.

(50) van der Spoel, D.; Berendsen, H. J. C.; van Buuren, A. R.; Apol, M. E. F.; Meulenhoff, P. J.; Sijbers, A. L. T. M. *Gromacs User Manual*; Nijenborgh 4, 9747 AG Groningen, The Netherlands, 1995.

(51) Car, R.; Parrinello, M. *Phys. Rev. Lett.* **1985**, *55*, 2471−2574.

(52) Pasquarello, A.; Laasonen, K.; Car, R.; Lee, C.; Vanderbilt, D. *Phys. Rev. Lett.* **1992**, *69*, 1982−1985.

(53) Laasonen, K.; Pasquarello, A.; Car, R.; Lee, C.; Vanderbilt, D. *Phys. Rev. B* **1993**, *47*, 10142−10153.

(54) Tassone, F.; Mauri, F.; Car, R. *Phys. Rev. B* **1994**, *50*, 10561−10573.

(55) Dal Corso, A.; Pasquarello, A.; Baldereschi, A.; Car, R. *Phys. Rev. B* **1996**, *53*, 1180−1185.

(56) Perdew, J. P.; Burke, K.; Ernzerhof, M. *Phys. Rev. Lett.* **1997**, *78*, 1396−1397.

(57) Vanderbilt, D. *Phys. Rev. B* **1990**, *41*, 7892−7895.

(58) Palma, A.; Pasquarello, A.; Car, R. *Phys. Rev. B* **2002**, *65*, 155314.

(59) Meloni, S.; Palma, A.; Kahn, A.; Schwartz, J.; Car, R. *J. Am. Chem. Soc.* **2003**, *125*, 7808−7809.

(60) Beljonne, D.; Cornil, J.; Friend, R. H.; Janssen, R. A.; Bredas, J. L. *J. Am. Chem. Soc.* **1996**, *118*, 6453−6461.

(61) Matsukawa, N. N.; Ishitani, A.; Dixon, D. A.; Uda, T. *J. Phys. Chem. A* **2001**, *105*, 4953−4962.

(62) Casida, M. E.; Jamorski, C.; Casida, K. C.; Salahub, D. R. *J. Chem. Phys.* **1998**, *108*, 4439−4449.

(63) Cosgrove, S. A.; Guite, M. A.; Burnell, T. B.; Christensen, R. L. *J. Phys. Chem.* **1990**, *94*, 8118−8124.

(64) Spezia, R.; Zazza, C.; Aschi, M. Manuscript in preparation.

(65) Toniolo, A.; Granucci, G.; Martinez, T. J. *J. Phys. Chem. A* **2003**, *107*, 3822−3830.

(66) Warshel, A.; Chu, Z. T. *J. Phys. Chem. B* **2001**, *105*, 9857−9871.

(67) Amadei, A.; D'Abramo, M.; Zazza, C.; Aschi, M. *Chem. Phys. Lett.* **2003**, *381*, 187−193.

(68) Laage, D.; Burghardt, I.; Sommerfeld, T.; Hynes, J. T. *J. Phys. Chem. A* **2003**, *107*, 11271−11291.

(69) Burghardt, I.; Laage, D.; Hynes, J. T. *J. Phys. Chem. A* **2003**, *107*, 11291−11306.